MODERN ARABIC REVIEW
of Fundamental & Applied Physics
Volume 1, N° 1 (2016) 44 -51

ANALYSIS OF THE MECHANICAL PROPERTIES OF ARC-SPRAYED COMPOSITE COATING USING MICROINDENTATION IN COMBINATION WITH INVERSE METHODS

Y. Fizi[a],
Y. Mebdoua[a],
H. Lahmar[a,b],
N. Ferguen[a],

[a]Centre de Développement des Technologies Avancées, Cité 20 août 1956, BP.17 Baba Hassen, Alger, Algérie.
[b]Laboratoire de physique Fondamentale et Appliquée, Faculté des Sciences exactes, Université Blida 1.

ABSTRACT

Elastic-plastic material properties for twin wire arc sprayed FeCNiBSi - (W/Ti)C coatings were investigated using modeling and experimental Vickers microindentation. SEM microstructure evaluations were also performed. The proposed methodology is based on the combination of Object Oriented Function (OOF2) and a nonlinear finite element analysis to extract the material properties described by Hollomon stress-strain relation.

KEY WORDS

- Arc spray,
- Vickers micrindentation,
- Object Oriented Function,
- Non linear finite element analysis.

1. INTRODUCTION

Arc-sprayed deposits are increasingly being used in a wide variety of industries. In order to understand, predict, and improve the reliability of coated devices, it is necessary to characterize their mechanical properties. The determination of the mechanical properties in thermal sprayed coatings is quite complicated, and often-contradictory mechanical properties are reported. Non-destructive experimental procedures have been increasingly used to determine the mechanical properties of materials. In particular, instrumented indentation tests have been used to measure the depth of penetration of an indenter into a test piece. The results of such tests can be used not only to obtain and to interpret the hardness of the material but also to provide information related to near surface mechanical properties and the deformation behavior of bulk solids and coating. Instrumented indentation technique emerges as an attractive technique for measuring the mechanical properties of materials of small volume, and it is convenient, quick, and inherently simple without extensive effort of sample preparation in comparison with conventional tensile or compression experiments [14-]. An instrumented indentation test (IIT) allows local properties identification.

Various approaches have been proposed to determine the material properties of power law materials using dimensionless analysis and the concept of a representative strain, based on the forward and reverse algorithms. In the literature, the values of representative plastic strain vary over a broad range and most of those values are calculated from curve-fitting approaches, rather than being based on physical relationships. Using the dimensionless analysis, most approaches use analytical functions, which critically depend on the accuracy of fitting, and limit the range of materials to which they may be applied. In recent years, a number of methods based on both experimental and numerical studies have been proposed to extract the elastic-plastic properties from the indentation data.

Finite element analysis (FEA), based on domain discretization, was developed to analyze indentation test. Dao et al. [1] and Bucaille et al. [5] used FEA to study instrumented sharp indentation and proposed analytical expressions of elastoplastic properties based on the FEA results. For example, Cheng and Cheng [6,7] used dimensional and finite element analyses to evaluate the mechanical properties of the materials from conical indentation problems.

An alternative method based on displacement and energy approaches to determine Young's modulus, yield strength, and hardness from the loading part of the indentation curve and the indentation depth after unloading was also proposed in the work of Giannakopoulos and Suresh [8].

Microstructures of thermally sprayed coatings are complex with inclusion of pores, cracks and different material phases. Few researchers have therefore attempted to simulate the correlation between a thermal spray microstructure and mechanical properties of these coatings [9]. The complexity of a thermal sprayed microstructure makes it difficult to model and simulate the classical techniques and thus very appropriate for this approach.

In this paper instrumented micro-indentation and meshing in the Object Oriented Finite Element 2 (OOF2) program was combined with a nonlinear finite element analysis to determine elastic-plastic properties of an arc sprayed composite coatings. To generate a FE-mesh from such an image, the software OOF2, from the United States National Institute of Standards and Technology (NIST), is used. This software was developed to investigate the behavior of microstructures. OOF2 takes a non-reductionist approach to build a data structure on the digitized image of the microstructure whereby it is connected to the associated material properties. Three elastic-plastic parameters (modulus young's E, yield stress and work hardening exponent n) are extracted, in a non-linear optimization approach, fully integrated with FE analysis, using results from a single indentation curve. The iteration procedure for optimization is based on MATLAB® nonlinear least-squares, where a result file is created to automatically update the plastic material properties of a power-law material in the ABAQUS® input file and then run ABAQUS® to obtain a loading- unloading curve, which is then compared to experiment data curve.

2. EXPERIMENTAL PROCEDURE

2.1 Sample Fabrication

In this research study, a twin wire arc spraying (TWAS) (ARCSPRAY 234-Metallization Company) was employed to spray FeCNiBSi-(W/Ti)C coatings. The Metco 8297 cored wire with a diameter of 1.6 mm (Sulzer Metco, Switzerland) was used as wire feedstock material. The wire is Fe-based based amorphous alloy matrix with inclusions of tungsten carbide and titanium carbide. The morphology of the wire used for this investigation is shown in Fig. 1. A total coating thickness of 460 µm was sprayed on a C35 substrate. The coatings were sprayed on grit blasted and cleaned carbon steel substrate cylindrical form with 25 mm in diameter and 5mm in thickness applying a voltage of 30 V, a current of 220 A, and air pressure of 6 bar with a spraying distance of 140mm.

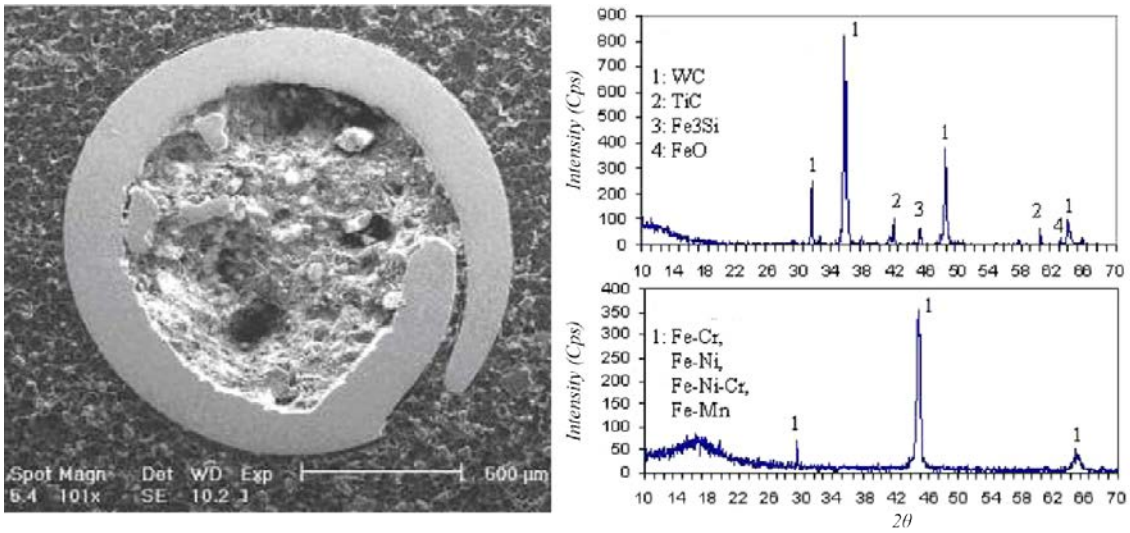

Fig. 1. SEM image and RX specters of the cored wire section (Sheath-powder) [10].

2.2 Metallographic Investigation

X-ray energy dispersive spectroscopic (EDS) and SEM observations of the coating microstructure studies revealed the presence of porosity and oxides, it can be seen that all coatings consisted of lamellas built up from composite splats with inclusion of unmolten particles. The carbides are also bounded with these Fe-rich phases. The exposed Fe-rich surfaces however were in contact with oxygen at high temperature, resulting in surface oxide layers around the particles, which became incorporated into the coatings, as shown in figure2(a). The oxide layers can be clearly seen as dark gray layers between the lamellae and porosity as black spots (Figure 2.(b)). La Barbera-Sosa et al. [11] showed that the amount of unmolten particles and the presence of pores and cracks between lamellae are inversely affected by the increase of the spray distance. The EDS analysis of the coating in Fig. 3 exhibits the dissolution of W, Ni and Cr in Fe-rich phases. The interface between the coating and substrate is compact with no voids or detected delamination.

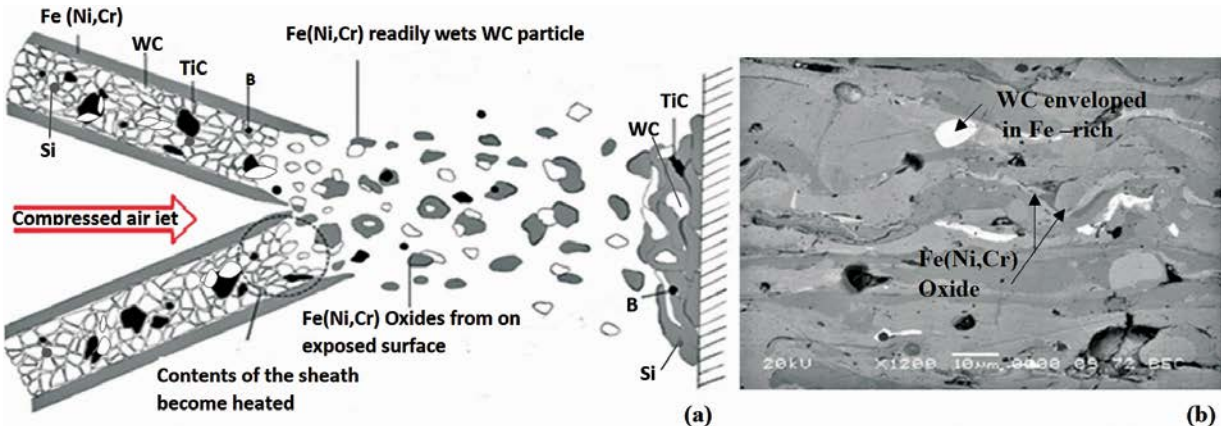

Fig. 2. a) Schematic diagram showing the physical actions of sprayed particles during the EAS process, b) Micrographs of coating

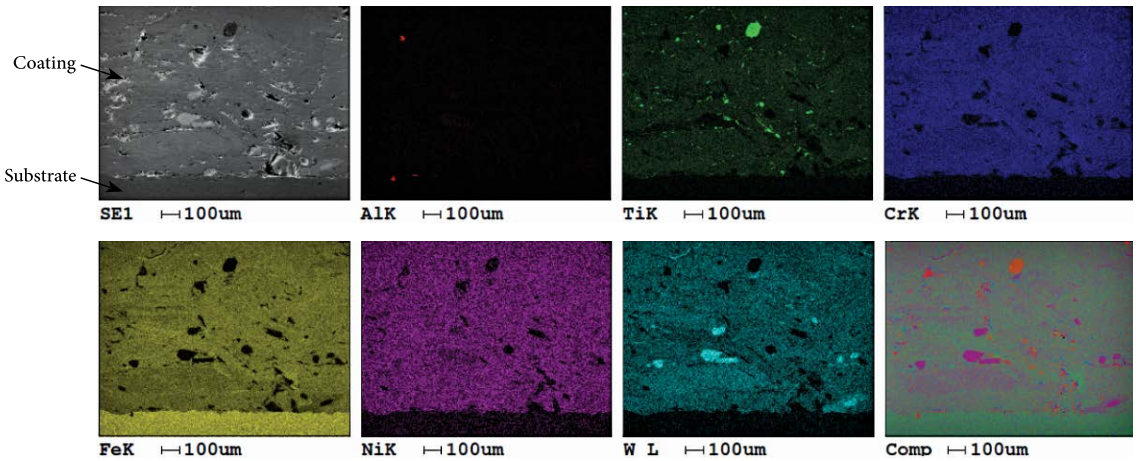

Fig. 3. EDX analysis of an arc-sprayed composite coating

2.3 Mechanical Characterization

Indentation Test

To explore the feasibility and robustness of the optimization algorithm in real-life applications, it is appropriate to consider an experimental load–displacement curve test to extract the material properties. In this case, experimental load–displacement curves for composite coating used in this study are based on microindenter Z2.5 with a Vickers tip.

A Zwick/Roell equipment, with a resolution of ± 0.01% in force and 0.02 µm in displacement, was used. The experiment is displacement controlled with an indentation velocity of 8.3µm/s. When the maximum available depth was reached, the indenter was held for 15 seconds, and then moved back with the same velocity. A Vickers indenter with a maximum load of 5N was used. The load-displacement curve was recorded continuously and elastic modulus determined from the unloading curve according to the Oliver and Pharr method.

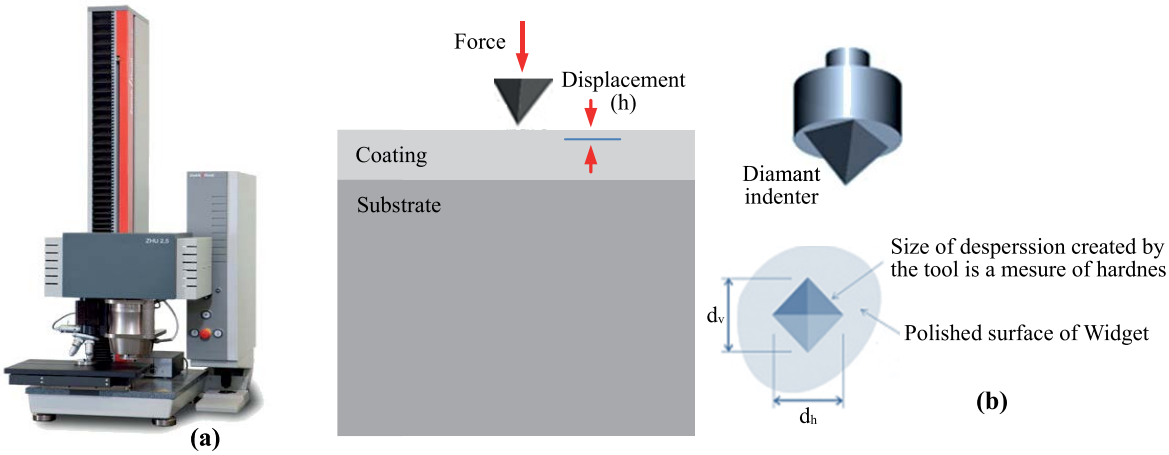

Fig. 4. Z2.5 Zwick indentation device (a) Schematic illustration of micro-indentation on a thermal sprayed coating. (b)

3. ANALYSIS PROCEDURE

The plastic properties of the coatings were determined by solving the inverse problem using a two-dimensional finite element analysis (FEA) model. For this purpose, the determined elastic modulus was given as input in the FEA model with a stress-strain curve first assumed as an initial constitutive relation for the coating. A load-displacement curve was then predicted using the model. The predicted load-displacement curve was then compared with the experimental load-displacement curve, and the constitutive curve was iteratively modified until a best fit is reached.

4. FEA MODEL

In this study, the finite element simulations were performed using the commercial finite element code ABAQUS®. Contacts between indenters and composite coating are modeled. The methodology to create such a model is based on three independent steps. In the first step a digital microstructure cross section is made. In the second step this image is imported into the object-oriented finite-element analysis program OOF2 and a mesh constructed. The last step considers development of a nonlinear elastic-plastic simulation model of micro-indentation in the finite element software ABAQUS®.

4.1 The OOF2 Model

Construction of Finite Element Models from Real Micrographs

The OOF2 model was created from an image of a microstructure cross-section. Polished sections were therefore prepared for microscopy analysis. The microstructure image was determined with an SEM. The digital image of the cross-section, consisting of 304x291 pixels, was imported into the program OOF2; an object oriented finite element program, developed at the Centre for Computational and Theoretical Material Science (CTCMS) at NIST. A typical cross-section is shown in Figure 5. The dark areas in Figure 5 (b,c) represent pores and micro-cracks, while the light areas correspond to the Fe-rich phase material.

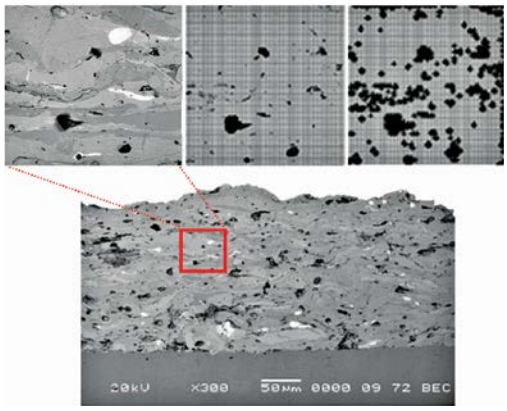

Fig. 5. *Typical examples of OOF models based on SEM morphological images of composites coating*

4.2 Indentation model

Instrumented indentation was performed using the finite element software ABAQUS®. The overall objective with the FEA model is to predict the elastic-plastic material behavior, namely, stress-strain relationship based on load-displacement relationships determined through indentation, that is, through inverse analysis. The two meshes created in OOF2 were written in Abaqus format. The sample was modeled using a two-dimensional axisymmetric mesh Modeling. Contacts between indenters and composite coating were modeled. The Vickers indenter was modeled with semi-vertical angle of 68°. At the very tip of the indenter, a spherical rounding with a radius of 5 µm was constructed because of the fact that no real indenter can be ideally sharp. During the loading step, the rigid cone indenter moves downwards along the z-direction and penetrates the foundation up to the maximum specified depth. In the second step, the indenter then as taken back to the initial position. The contact between the indenter and the material is assumed to be perfect and without friction. The nonlinear problem is caused by three different effects: large strains under the indenter necessitate frequent updates to all nodes in the mesh, material properties are nonlinear due to plasticity, and contact between the indenter and the sample produces nonlinear boundary conditions. The boundary conditions were specified in the following way. First, along the horizontal bottom line of the sample, the displacements (ux) were set to zero. Then, along the axis of symmetry, that is, the left side of the sample, nodes were constrained to move along the axis of symmetry only (uy = 0). The indenter (Fig. 3) moves downward by 6.42µm per second. Rigid body movement was constrained in all other directions.

4.3 Material model

The elastic behavior is modeled by the elastic modulus. The plastic behavior of the materials used in the numerical simulations was modelled considering the stress and plastic strain, a power law strain hardening curve has been used. The stress-strain ($\sigma - \varepsilon$) relationship [12] is assumed to be :

$$\sigma = \begin{cases} E\varepsilon & for\ \sigma \le \sigma_y \\ E\varepsilon^n & for\ \sigma > \sigma_y \end{cases} \quad (1)$$

where K is a strength coefficient. Considering continuity at the initial yield point,

$$\sigma_y = E\,\varepsilon = K\varepsilon^n \quad (2)$$

Such that : $K = E^n \sigma_y^{1-n}$ (3)

In ABAQUS® input file, a discrete set of points was required to represent the uniaxial stress–strain data, rather than specifying the work-hardening exponent n. Therefore, the set of plastic strain values varied from 0 to 0.2 with an increment of 0.02 in order to specify the plastic stress–strain data in ABAQUS®. The friction coefficients at the contact between the indenter and the top surface of the bulk material were assumed to be zero, since friction had a negligible effect on the indentation process [5]. The presence of the substrate material was ignored in the analyses, as the indentation depth was shallow enough to regard the influence of the substrate material.

Application of inverse analysis in indentation problem

There are four material parameters, namely, E, σ_y, n and υ, to be defined for an elastic–plastic material behavior. For simplicity, the value of Poisson's ratio (υ) for composite is assumed to be 0.3. A number of optimization techniques have been used elsewhere [13-15] to determine material properties from indentation load–displacement curve tests. In this study, a non-linear optimization technique is devised within the MATLAB®, which provides an excellent interface to FE codes such as ABAQUS®. The inverse analysis based on Levenberg-Marquardt (LM) method is used to estimate two material properties. The LM method is described extensively in [16] and its use within the context of this work is illustrated by the flow chart shown in Figue.7. Essentially, it processes the experimental data and attempts to obtain the best estimates for unknown state variables based on least-squares theory. The inverse analysis is based on the minimization of a cost functional measuring the discrepancy between the measured data and the one computed from the direct problem model. The expression of this cost functional for the indentation test can be expressed as in Eq. (4).

$$J(U) = \tfrac{1}{2}\sum_{i=1}^{N}\left[F_i^{comp}(U) - F_i^{meas}\right]^2 \quad (4)$$

Where $F_i^{comp}(U)$ and F_i^{meas} are respectively the reaction forces on the indenter obtained from measurement and computation of the direct problem. U is a vector that contains the unknown parameters, $U^T = \left[E, \sigma_y, n\right]$ and N is the number of measurements.

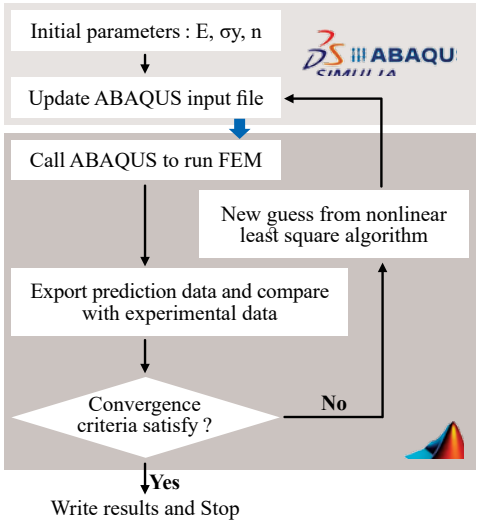

Fig. 6. Flow chart of the optimization algorithm used to determine the mechanical properties

5. RESULTS AND DISCUSSION

Experimental results

The depth-sensing indentation measurements are used to determine the hardness and the Young's modulus. The Oliver-Pharr method [17] was used to determine the elastic modulus. The reduced modulus is related to the specimen modulus through :

$$\frac{1}{E_{IT}} = \frac{(1-\nu)_s^2}{E_s} + \frac{(1-\nu)_i^2}{E_i} \quad (5)$$

Where E and are the Young's modulus and the Poisson's ratio, respectively, of the specimen (s) and of the indenter (i). Table 1 shows the ten reduced E-moduli calculated from the indentation experiments.

Table 1. Mechanical properties measured from the IIT

Properties	HIT N/mm²	EIT kN/mm²	dh µm	dv µm	HV
Results	4846±38	78,41±52	39.44 ± 1.4	40.68± 0.9	577.76 ± 06

Two experimental indentation curves, corresponding to maximum and minimum values of determined E-modulus are shown in Figure 4. The Two curves coincide at the beginning but deviate at the high force points, this may be due to micro-cracks, which could be created progressively under the indenter when the load increases. Also, probably for the same reason, the penetration depth of the indenter increases with porosity.

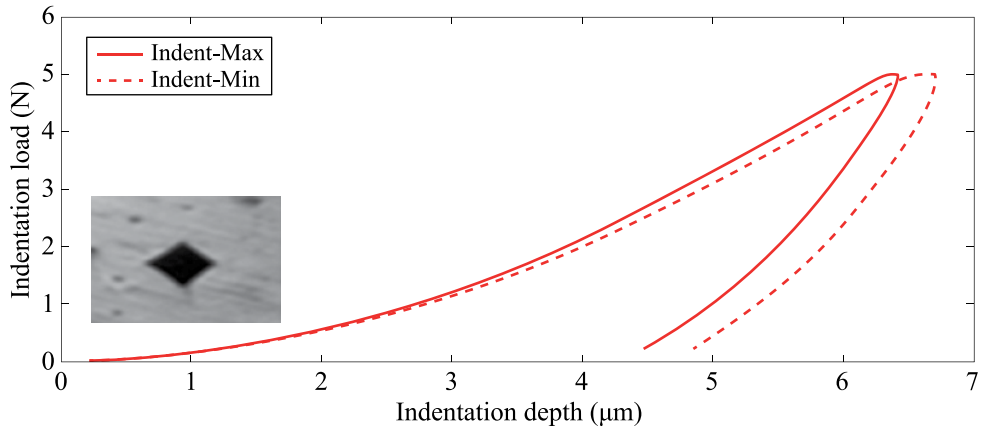

Fig. 7. Experimental results from indentation tests corresponding to maximum and minimum values of the E-modulus.

Simulation results

Finite Element Analysis

Modeling instrumented indentation was performed using the finite element software ABAQUS®. The specimen was modeled as an axisymmetric geometry with four-node axisymmetric quadrilateral continuum elements with reduced integration (CAX4R). The specimen was meshed with a total of 1818 axisymmetric elements. A fine mesh density was used around the area of contact indenter coating, this density became coarser as one moves away from this zone. The Arbitrary values of E, σ_y and n, have been chosen as initial values and the optimization algorithm has been used to find the optimized parameter from which the best fit between the experimental and predicted load–displacement loops can be achieved.

The objective function is the error in the force-depth curves between the experiment and FEA. Figure 9 shows the force-depth curve from the experiment and the simulation with the initially and optimum material properties. The material parameters that lead to the best fitting agreement can be considered to represent the constitutive behavior of the coating. This simulation result is observed after nine iteration, in this case, the law of modelled behavior is defined by $\sigma_y = 1{,}69\ GPa$ and n = 0,38. It is worth mentioning that these parameters varied, depending on the position analyzed and the associated experimental data. Experimental and numerical study [18] shows that stress–strain estimated curve can be approximated by Ludwick law ($\sigma = \sigma_y + K\varepsilon_n^p$). Table 2 shows the comparison between the results of the identification procedures of Hollomon and Ludwig laws.

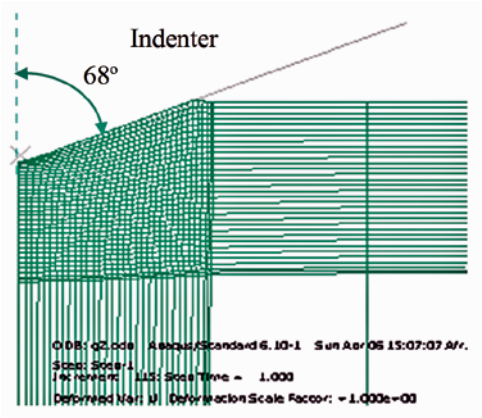

Fig. 8. Deformed configuration at maximum penetration depth in the proximity of the indenter

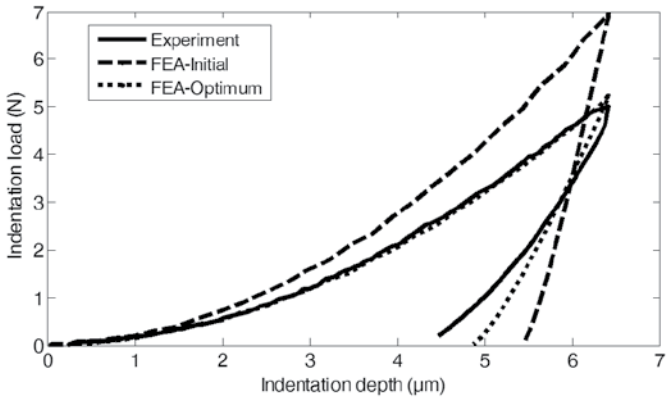

Fig. 9. Comparison between experimental and simulation data for indentation curve, initial and optimized results

Table 2. Results of the identification procedures

Ludwik model [18]					Hollomon model		
$E(GPa) = E_{exp}$	σy (MPa)	K (GPa)	M		E (GPa)	σy(MPa)	N
137.02	1700	3.08	0.29		122.04	1691.80	0.38

Object-Oriented Finite Element Analysis

Two OOFEA indentation curves derived in this study corresponds to model EF1 and model EF2 are shown in Figure11. Both curves show the oscillation at the beginning of the loading step. This oscillation can be explained by the mesh density used around the contact indenter-coating. The simulated load-displacement relationship using a homogeneous mesh, OOF simulated load-displacement are shown in Figure 12, and compared with the experimental results. A good agreement between the experimental curve and corresponding predicted curves can be seen.

The maximum reaction force from FEA is slightly higher than the experimental data. In addition, there are differences between the experimental data and FE solutions at the end of unloading portion and it is expected that the accuracy of the optimization results will be affected by these differences. A contrario, an analysis based on the OOF mesh, a better fit at unloading can be seen. The optimization results are summarized in Table 3 where the sensitivity of the proposed algorithm is demonstrated by changing three parameters at a time.

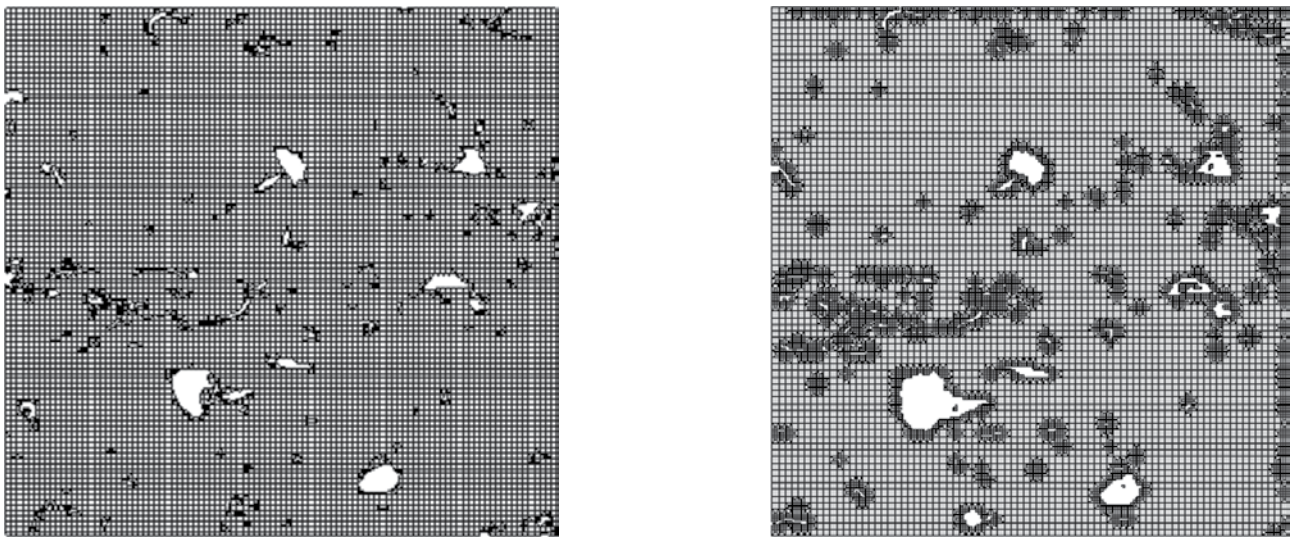

Model EF1 (a) Model EF2 (b)

Fig. 10. Finite element simulation model of composite coating (a) refine mesh, (b) snap refine mesh

It is well known that Vickers hardness HV is about 3σ0.08, which corresponds to about three times of the flow stress at ε=0.08(8%) [1,19]. This means that the measured HV can predict one point on the stress and strain curve (the flow stress of σ0.08). This HV measurement yields the σ0.08 of 1925.86 MPa. The estimated stress–strain curve with OOEFA-1gives us σ0.08 of 1813.55MPa, showing the good agreement to each other. Thus, the present approach for stress–strain behavior estimation is validated by this HV measurement. The material parameters that defined by this analysis (OOFEA-1) represent the behavior of the coating.

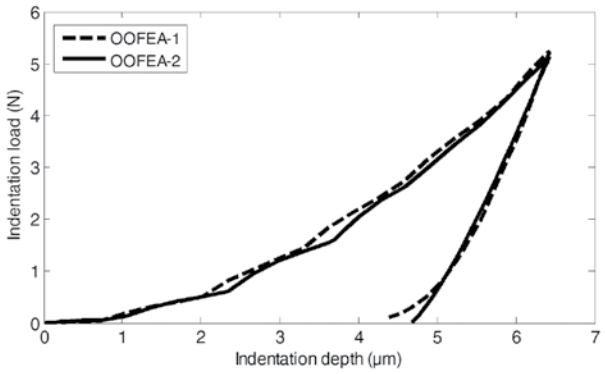

Fig.11. Indentation response of composite coating by object-oriented finite element analysis

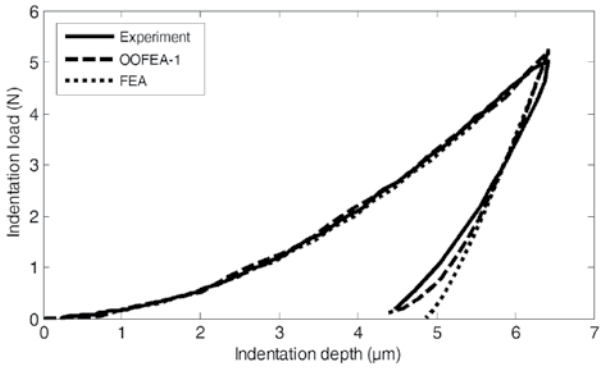

Fig. 12. Comparison between experimental and simulation data for indentation curve, FEA and OOFEA results

Table 3 : Three-parameter optimization for FEA and OOFEA

FEA				OOFEA-1				OOFEA-2		
E (GPa)	σ_y (MPa)	n		E (GPa)	σ_y (MPa)	n		E (GPa)	σ_y (MPa)	n
122.04	1691.80	0.38		87.29	904.38	0.32		111.80	1499.80	0.33

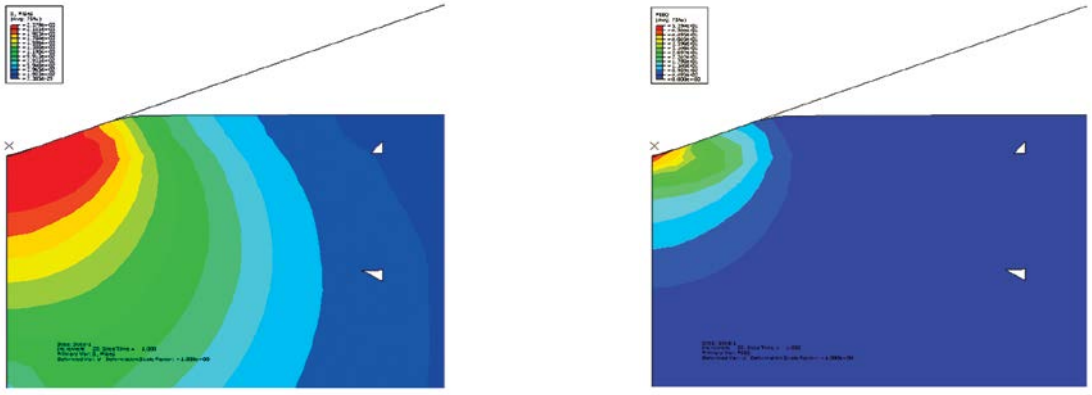

(a) (b)

Fig. 13. Simulated von Mises stress distribution (a) and equivalent plastic strain under the indenter (b)

Three-dimensional Vickers model

For comparison of the optimization technique, 3D quarter-symmetry FE models for the Vickers indenters are also used; In this case, the stress-strain curve estimated with OOFEA-1 is used to simulate the micro-indentation test. In addition to the symmetry constraints on the symmetry planes, the bottom of the specimen is fully constrained. The specimen is modelled as three-dimensional geometries with a high element density of C3D8R in ABAQUS. For the rigid indenters, a four-node R3D3 is used. The loading and unloading procedures are the same as in the axisymmetric model. Example of simulation results are shown in Figure 14, and compared with the experimental results. The simulated load-displacement curve and the experimental one coincide at the low forces, but deviate at higher forces. The equivalent stress distribution of composite coating after loading is shown in Fig. 15. Stress concentrations at the indenter tip can clearly be seen.

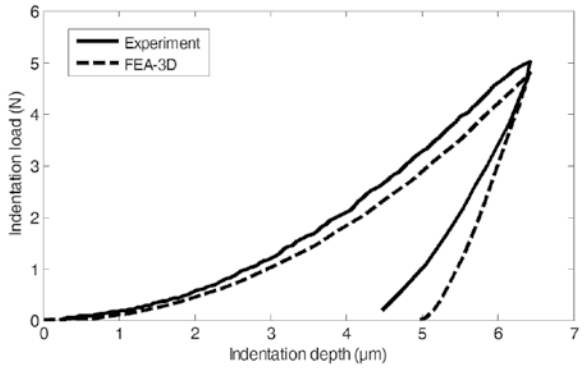

Fig.14. Comparison between experimental and simulation data of indentation curve with the indentation depth of 6.42 μm.

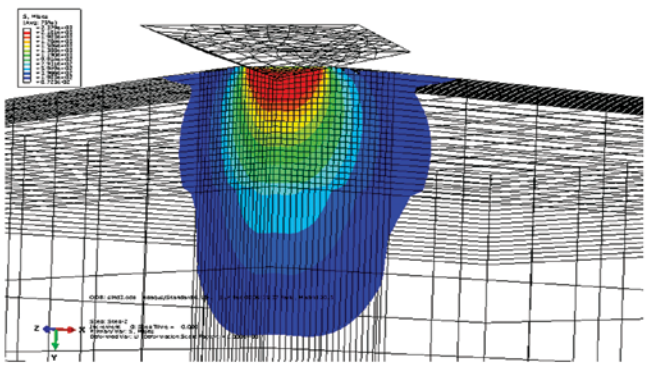

Fig. 15. Equivalent stress contour plot for composite coating after loading step (MPa)

5. SUMMARY AND OUTLOOK

TWAS-sprayed FeCNiBSi-(W/Ti)C coatings have been evaluated with regard to their mechanical properties. In this article, the coating was investigated using micro-indentation tests. The analytic Oliver-Pharr method was used to determine the Young's modulus of local points. With SEM and EDX analysis, the material composition was identified. A mechanistic approach was proposed for extracting the mechanical properties of the cored composite coating.

The approach was based on the combination of micro-indentation experiment, finite element and inverse analysis techniques. In a future work, it should be interesting to develop and evaluate a methodology based on the combination of OOF and a nonlinear finite element analysis to simulate the interfacial indentation test.

REFERENCES

[1] Dao, M., Chollacoop, N., Van Vliet, K. J., Venkatesh, T. A., and Suresh, S., 2001, "Computational Modeling of the Forward and Reverse Problems in Instrumented Sharp Indentation," Acta Mater., 49(19), pp. 3899–3918. [2] N. Ogasawara, N. Chiba, X. Chen, Mech. Mater 41 (2009) 1025–1033.

[3] A. Yonezu, H. Akimoto, S. Fujisawa, X. Chen, Mater. Des. 52 (2013) 812–820.

[4] B. Xu, X. Chen, J. Mater. Res. 25 (2010) 2297–2307.

[5] Bucaille, J. L., Staussb, S., Felderc, E., and Michler, J., 2003, "Determination of Plastic Properties of Metals by Instrumented Indentation Using Different Sharp Indenters," Acta Mater., 51(6), pp. 1663–1678.

[6] Cheng, Y. T., and Cheng, C. M., 1998, "Scaling Approach to Conical Indentation in Elastic-Plastic Solids With Work Hardening," J. Appl. Phys., 84,3, pp. 1284..

[7] Cheng, Y. T., and Cheng, C. M., 1999, "Scaling Relationships in Conical Indentation of Elastic-Perfectly Plastic Solids," Int. J. Solids Struct., 36, pp. 1231–1243.

[8] Giannakopoulos, A. E., and Suresh, S., 1999, "Determination of elastoplastic properties by instrumented sharp indentation," Scr. Mater., 40, pp. 1191–1198.

[9] Michlik, P. and C. Berndt, Image-based extended finite element modeling of thermal barrier coatings. Surface and Coatings Technology, 2006. 201(6): p. 2369-2380.

[10] S. Nourouzi, Contribution a l'etude du procede arc-fil pour la realisation de depôts metalliques durs resistants a l'usure abrasive. Thèse de doctorat, Universite de limoges, 2004.

[11] J.G. La Barbera-Sosa,Y.Y. Santana, E. Moreno, N. Cuadrado, Effect of spraying distance on the microstructure and mechanical properties of a Colmonoy 88 alloy deposited by HVOF thermal spraying. Surface & Coatings Technology 2010, 205, p.1799–1806

[12] DieterGE.Mechanicalmetallurgy. NewYork:McGraw-Hill;1976.

[13] G. Sun, F. Xu, G. Li, X. Huang, Q. Li,Determination of mechanical properties of the weld line by combining micro-indentation with inverse modeling.Computational Materials Science 2014,85,pp 347–362

[14] V. Buljak, M. Bocciarelli, G. Maier, Mechanical characterization of anisotropic elasto-plasticmaterials by indentation curves only.Meccanica, 2014,49,pp 1587–1599

[15] C.K.S. Moya, M. Bocciarelli, S. P. Ringerc, G. Ranzia, Identification of the material properties of Al 2024 alloy by means of inverseanalysis and indentation tests, Materials Science and Engineering 2011, A 529, pp 119–130

[16] D.S. Schnur, N. Zabaras, An inverse method for determining elastic material properties and a material interface, Int. J. Numer. Methods Eng. 33 (1992) 2039

[17] Oliver, W.C., Pharr, G.M., 1992. An improved technique for determining hardness and elastic-modulus using load and displacement sensing indentation experiments. Journal of Materials Research 7 (6), 1564–1583.

[18] Y. Fizi, Y. Mebdoua, H. Lahmar,S. Djeraf, S. Benbahouche,Adhesion of FeCrNiBSi–(W–Ti)Cwire-arc deposited coatings onto carbon steel substrates determined by indentation measurements and modeling.,Surf. Coat. Technol. 2014

[19] D. Tabor, Hardness of Metals, Charendon Press, Oxford, 1951.

ings Technology 202.2008